ARTICLE

Controlled Hydrothermal Pore Reduction in Anodic Alumina Membranes

D Mattia,[a] and H. Leese[a]

Porous anodic aluminium oxide nanostructures are popular templates for the fabrication of a wide range of nanomaterials. When open at both ends, they are now being used as model membranes, called anodic alumina membranes (AAM). In both cases, their appeal resides in the possibility of accurately controlling pore size via the anodization voltage, with a narrow size distribution. This characteristic, though, is maintained only in specific pore size ranges, reflecting specific ordering regimes in the material. Outside these domains, less ordered structures are obtained. Furthermore, the smallest pores currently achieved by anodization are about ~10 nm in diameter, using sulphuric acid, which yields very thin and fragile nanostructured membranes. In this work we address these limitations by decoupling the control of pore size from the anodization stage. We achieve this by subjecting AAMs produced under a high order regime (40 V, 0.3 M oxalic acid) to a post-anodization hydrothermal treatment using steam. With this process we were able to decrease the pore size by 80% down to ~10 nm. The membranes retain their integrity and are more robust that AAMs with the same pore structure produced via anodization in sulphuric acid.

Introduction

The formation of ordered oxide structures upon the electrochemical anodization of aluminium, first discovered in the 1940's, has become, in the last 15 years, a common tool of nanotechnology. The regular pore size, which is controlled via the anodization parameters, the narrow pore size distribution and cylindrical pore geometry, with constant cross-section,[1] have made anodic aluminium oxide (AAO) films ideal templates for the fabrication of aligned 1D nanostructures, including nanotubes, nanowires and nanorods.[2-4] While the mechanism at the onset of pore formation is still a matter of debate,[5] the formation mechanism of cylindrical pores is widely understood to be the result of competing reactions, the formation of aluminum oxide at the metal/oxide interface and the field-enhanced oxide dissolution at the oxide/electrolyte interface.[6] As the oxide formation is isotropic, the pores have a circular cross-section and terminate with a hemispherical oxide structure, known as the barrier layer. This can be removed to obtain open-through pores. As this is done using strong acid solutions capable of dissolving alumina, control of this process is crucial to prevent pore widening or even the dissolution of the entire membrane. A simple electrochemical method capable of tracking the passage of an electrolytic solution through the barrier layer as the pore opens can be used to precisely control this process.[7, 8] The result is the formation of freestanding structures, which have become popular as model membrane systems that can be used to study the effects of nanoscale confinement on fluid flow,[8-11] wetting behaviour,[12, 13] surface friction,[14, 15] or for nanoparticle synthesis.[16, 17] In this configuration, they are usually defined as anodic alumina membranes (AAMs).

As templates or membranes, these materials suffer from some important limitations, including reduced mechanical stability and, more importantly for the present work, specific anodization parameter (voltage, electrolyte type and concentration, temperature, time) domains where the pore structure is at a maximum order.[1, 18] Outside these parameter domains, this regularity is partially lost, with the creation of highly non-circular pores,[19] pore branching,[10] and/or defects in the hexagonal array structure.[5] In both cases, a linear relation between pore size and anodization voltage is observed with a proportionality constant of ~ 1.25 nm V^{-1}.[5, 12] This linear relation holds true even when the voltage is varied during the anodization, resulting in pores with varying diameter.[20] This linear relation, though, breaks down below 10 nm, where it is no longer possible to obtain highly regular structures.[18] Smaller pores have been obtained by reducing the anodizing voltage towards the end of the anodization process, leading to the formation of asymmetric structures, with pores below 10 nm at one end and larger pores at the other.[21] This approach, though, introduces branching in the pores and reduces the overall order of the porous structure.[10] In addition, to obtain the smallest pores requires the use of sulphuric acid, which is a powerful

etchant for alumina. As the thickness of the AAMs is related to the anodization time, there is a trade-off in play whereby the AAMs with the smallest pores have to be very thin (20-30 µm) to avoid pore widening by acid etching, resulting in a brittle structure.

In trying to overcome these limitations, other methods to produce smaller pores have been developed. In particular, efforts have been placed on the pore opening step to achieve a controlled partial opening of the barrier layer. Methods include the electrochemical pore opening setup discussed earlier,[7] bulk wet chemical etching,[22] or an ion-beam to drill individual holes.[23] All these methods, though, produce asymmetric structures, with no effect on the pore diameter beyond the barrier layer. Considering the relatively small range of pore sizes where the optimal structure is conserved and the lower limit on pore sizes achievable, alternative methods to decrease pore size uniformly throughout the length of the pore and without decreasing the quality of the pore structure would be very useful both for templating and filtration applications.

The sealing of porous anodic alumina films via hydrothermal treatment has been used in industry since the 1950s and is still used routinely today to protect aluminium surfaces from corrosion, from window frames to electronic devices.[24] More specifically, the hydrothermal treatment in boiling water of nanoporous AAO films (i.e. with the barrier layer intact) has also been extensively studied to seal the porous structure,[25, 26] and increase its corrosion resistance.[27] The sealing occurs through a complex process involving the partial dissolution of the oxide pore wall in contact with boiling water, with concurrent re-precipitation of a swollen hydroxide gel, which leads to a decrease in pore size and eventually sealing.[28] The amount of water present in the closing pore directly affects the subsequent corrosion resistance as it changes the composition and mechanical resistance of the forming gel.[27] The chemical composition of the starting material (high purity Al or Al-alloys) and that of the electrolyte also have strong effects on the composition and mechanical stability of the plug.[29] It is well known that ions from the electrolyte are incorporated into the oxide layer being formed during anodization.[6] These can then be released during the hydrothermal process and be re-incorporated in the forming plug, affecting corrosion resistance and mechanical stability.[28]

In this work, three different hydrothermal treatments have been investigated to uniformly decrease the pore size of open-through AAMs. These include immersion in a boiling water solution, an electrochemical treatment and steam treatment. The latter produced a uniform pore reduction of 80% down to the 10 nm limit, throughout the pores' length.

Experimental

AAM Fabrication

The AAMs were prepared using the well-established two–step potentiostatic anodization process.[30] Details of the entire process are reported elsewhere.[8] Briefly, 10 mm aluminium (99.99%, 0.25 mm thickness, Alfa Aesar) disks were annealed in air (1 hour at 500 °C), cleaned by ultra-sonication in acetone and electropolished in a solution of ethanol/perchloric acid 1:4 solution (15 min at 20 V and temperature below 50 °C). The disks were then anodized in 0.3M oxalic acid at voltages ranging from 25 to 80 V, with temperature regulated between 13 and 0 °C, depending on the anodization voltage. The alumina layer formed from the one-hour first-step anodization was then removed by wet chemical etching using a 1:1 mixture of 6 wt% phosphoric acid and 1.8 wt% chromic acid at 60 °C for 20 min. The second anodization was performed immediately after under the same conditions as the first step, but for a longer period of 10 to 12 h. The residual non-anodized aluminium substrate was removed by immersion in a 1:1 solution of 0.2 M $CuCl_2$ to 20% hydrochloric acid. The oxide barrier layer was removed by contact with a 6 wt% phosphoric acid in an electrochemical setup to control the pore opening and prevent pore widening (Fig. 1a). The barrier layer side of the AAMs was placed in contact with phosphoric acid, whereas the open side was in contact with 0.2 M KCl solution. A current (under a 0.2 V external field) was detected when the pores started to open during etching.

Hydrothermal treatments

Three different hydrothermal processes were used in this work: First, the membranes were submersed in a vessel containing boiling water for 1 hour, in an attempt to reproduce the method used in the literature for AAOs. The vessel was placed on a hot plate and no stirring was used as the rising of the vapour bubbles generated at the base of the vessel in contact with the hot place created sufficient agitation. A variation of this method was to flow the boiling water through the AAMs for 1 hour using a peristaltic pump recirculating the boiling water.

Second, we modified the electrochemical setup used to evaluate pore opening to detect pore shrinkage (Fig. 1a). In this case, a 0.8 M NaCl solution was placed on both sides of the membrane and heated to 85-90 °C. An external field of 2.5 V was applied across the membrane sandwiched between the two vessels and the current generated was measured at periodic intervals.

Finally, we connected the membrane to the top of a sealed vessel sitting on a hot plate and containing boiling water using an U-shaped pipe (Fig. 1b). The steam from the flask was driven through the membrane and observed flowing out of the membrane. The steaming process was carried out between 5 to 40 minutes.

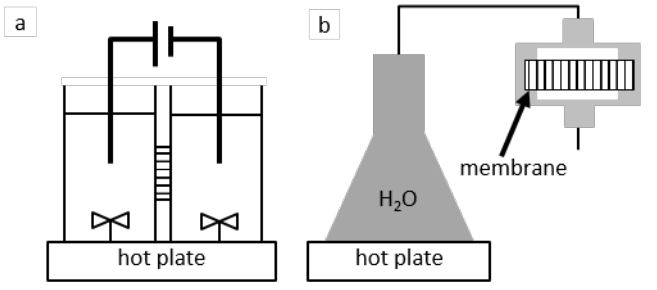

Fig. 1 a) Electrochemical setup for pore opening and pore reduction; b) steam treatment setup.

Membrane Characterization

The AAMs before and after each hydrothermal treatment were characterized using AFM (Digital Instruments Nanoscope IIIA), FESEM and FIB (Carl Zeiss XB1540 Gemini®).
The micrographs were statistically analysed using ImageJ software to obtain the pore structural characteristics, i.e. pore diameter, pore circularity, porosity and pore size distribution. Details of the analysis process are provided elsewhere.[8]

Results and Discussion

The as-produced AAMs have a regular pore structure with narrow size distribution and constant cross-section throughout the length of the membrane (Fig. 2), consistent with our previous reports.[8, 9, 12] The linear relationship between anodization voltage and pore size is also consistent with the value reported by us and others in the literature.[12]

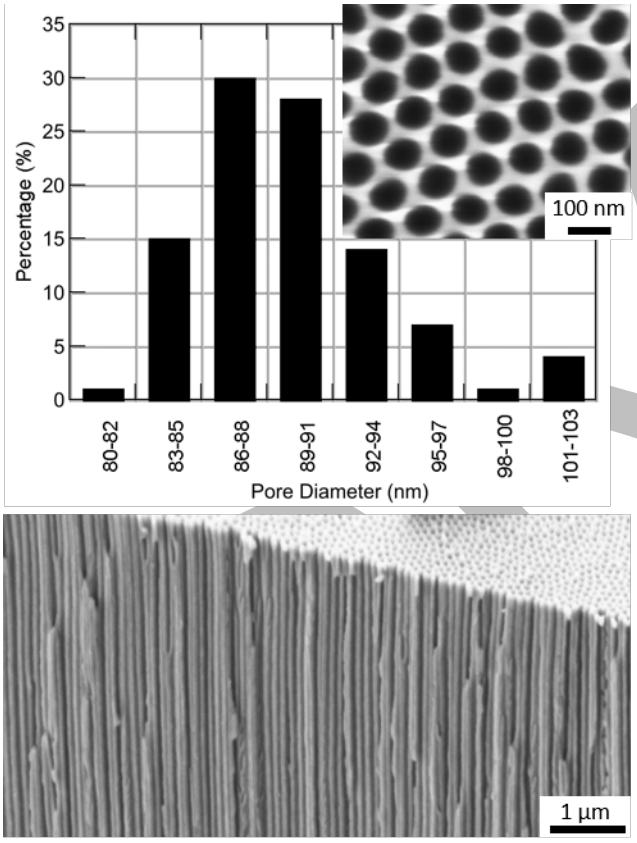

Fig. 2 AAM (a) pore size distribution (synthesis conditions: 70 V, 0.3 M oxalic acid, 0 °C); (b) SEM micrograph of the bottom side after pore opening; (c) SEM micrograph of the cross-section, obtained using an FIB, showing the constant cross-section throughout the length of the pores.

Boiling water treatment

The treatment in boiling water was first attempted to mimic the process used in the literature to seal the pores of AAO films (with the barrier layer still in place).[31] After 1 hour in hydrostatic conditions, a clear decrease in pore size was observed on both sides of the AAMs (Fig.s 3a and 3b), but inspection of the membrane cross-section revealed that the swelling of the pore wall was occurring at the pore mouth on either side of the membrane, with the rest of the pore length largely unaffected (Fig. 3c). In addition, the roughness of the membrane surface increases significantly. As in the case of the AAO films, the pore entrance starts swelling, leading to a reduction in pore size. In the case of the AAOs where only one side is open, the neck progressively restricts the entrance with more and more oxide depositing at the bottom of the pore. This plugging mechanism for AAOs is well-known,[31] and is attributed to the formation of boehmite (γ-AlOOH) or pseudo-boehmite, following a complex process: First, the initially dry oxide wall is hydrated, with H^+ and OH^- ions chemisorbed onto the surface. Subsequently H_2O is physically adsorbed onto the layer of the chemisorbed species, swelling the pore walls.[31]
In the present case, where the AAMs are open at both ends, necking at the pore entrance still occurs via the same chemical/physical adsorption process, but no accumulation is possible, resulting only in blocking at both entrances. Attempts to flow boiling water through an AAM using a peristaltic pump produced similar results, confirming that no accumulation in the pore section between the entrances occurs. The swelling is permanent, with the growth of secondary structures or roughness (Fig. 3).

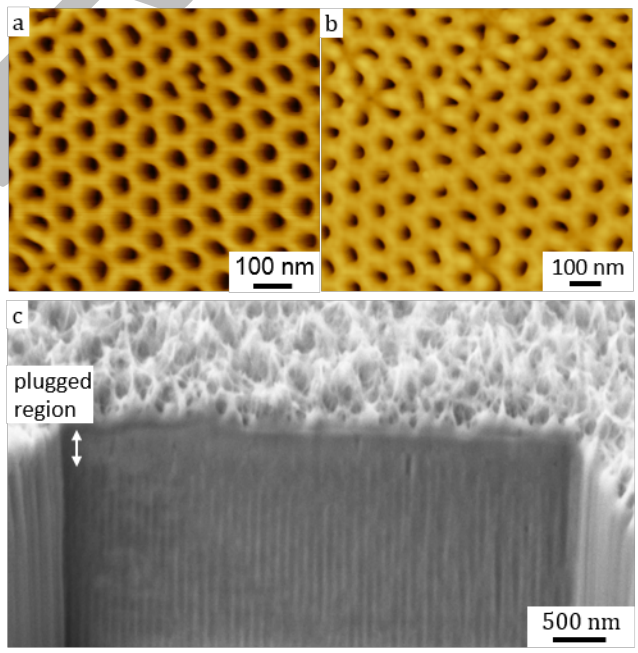

Fig. 3 AFM micrographs of an AAM top surface (a) before and (b) after treatment in boiling water for 1 hour. c) SEM micrograph of the cross-section of an AAM after 1 hour treatment in boiling water showing a significant increase in roughness at the membranes' surface plus a plugged region at the pores' mouth.

Electrochemical treatment

In an attempt to further understand the plugging mechanism observed for the boiling water treatment, the electrochemical

setup used to detect pore opening was modified to monitor pore reduction. Fig. 4 shows a composite plot of current variation with time during the pore opening and the pore reduction steps. In the former, current is measured until the barrier layer is etched away by the acid. Once there is a breach in the barrier layer, the current increases linearly as the pores widen. The process is normally stopped once a plateau in the current is reached. For the pore reduction experiment the acidic electrolyte was replaced with 0.8 M NaCl on both sides of the membrane. A current was measured from the start (the slight mismatch in Fig 4a is given by the different electrolytes used). A further increase was observed and expected while the setup was heated for the hydrothermal treatment. Once the temperature was reached, current started decreasing steadily, suggesting that indeed pores were closing.

Analysis of FESEM data showed a very different picture where the formation of fibrous structures was observed on both sides of the membrane (Fig. 4b). The fibres nucleation appears to be located in the interpore spacing on the two surfaces of the membrane (Fig. 4c). Even though the underlying porous structure appears to be preserved, the overall result is a progressive blocking of the pore mouths, explaining the observed reduction in current.

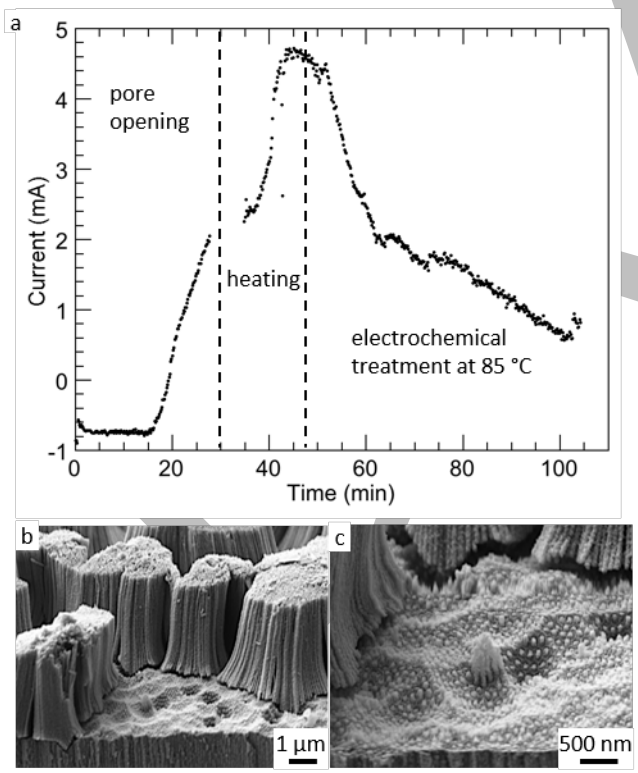

Fig. 4 a) Composite plot of the variation of the current over time during the pore opening (using phosphoric acid), and the pore reduction steps (using NaCl) in an electrochemical setup for a 40 V, 0.3 M oxalic acid AAM. SEM micrographs showing b) fibrous structure grown on the AAM's surface, with nucleation occurring in the interpore spacing (c).

Steam treatment

As a final method, the membranes were subject to a flow of steam for times ranging from 2 minutes to 23 minutes. For times shorter than 19 minutes, pore size decreased uniformly on both membrane surfaces (Fig. 5a and 5b), with no significant roughening of the surface, and throughout the whole pore length (Fig. 5c). The latter aspect can only be proven on a semi-quantitative basis, as the FIB treatment used to create the membrane cross-section is destructive. This means that it was not possible to observe the cross section of the same membrane before and after steam treatment. On the other hand, using AAMs produced in one of the highly ordered regimes (40 V, 0.3 M oxalic) ensures that AAMs with comparable average pore diameters are obtained consistently.

The pore size reduction increases with increasing steam treatment time up to 14 minutes (Table 1). Prolonging the steam treatment beyond that time led to growth of fibrous structures similar to those observed in the hydrothermal case. In the latter case the apparent reduction in average pore size is in fact due to the growth of fibres on the membrane surface that alters the image analysis results.

Table.1 Pore size reduction as a function of steam treatment time

Steam treatment time	Pore diameter (nm)		
(min)	before	after	reduction (%)
10	49±4	39±2	20
12	70±9	49±7	30
14	83±8	44±6	47
17	73±10	48±6	34

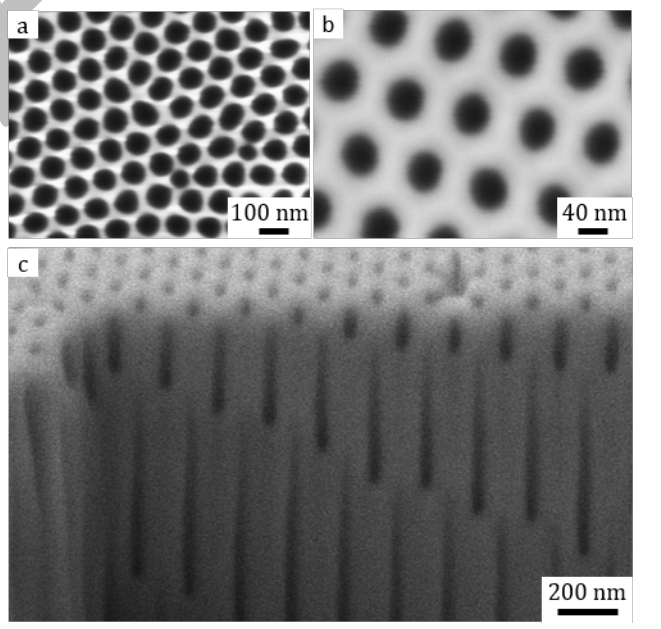

Fig. 5 SEM micrographs of an AAM (a) before and (b) after steam treatment for 12 minutes; c) SEM cross-section of AAM after steam treatment for 12 minutes showing uniform pore diameters throughout the membrane length and no roughening of the surface. The apparent alternating pore structure is an artefact of the FIB milling process.

To gain a more quantitative understanding of the pore reduction mechanism, a 40 V membrane (average starting pore size 50

nm) was subject to incremental amounts of steam treatment (Fig. 6). After each step, the AAM was analysed via AFM. After 16 minutes, a reduction of 80% is observed, down to 10 nm (Fig. 6d). This result is quite remarkable since, as discussed, 10 nm is the smallest pore size that can be achieved for a symmetric AAM. Furthermore, this small pore size cannot be achieved using oxalic acid but only using sulphuric acid. Since sulphuric acid has a high etching rate for alumina, AAMs with such small pores are very thin and, as a result, tend to be brittle and difficult to handle. In contrast, the present AAM was produced using oxalic acid, yielding a more robust membrane. The steam treatment allowed for a reduction in pore size, without compromising the quality of the nanostructure.

As in the previous case, prolonging the steam treatment led to the formation of a fibrous structure. As the steam treatment progresses, surface roughness also increased (Fig. 6c and 6d). Unlike the AAMs treated in boiling water, though, the roughness appears to be more uniform, due to isotropic growth of the oxide, forming what appear to be domed structures.[12, 15] Excluding the final point where fibres were observed, there is a linear relationship between pore reduction and time of steam treatment – with the slope equal to ~ 2.4 nm diameter reduction per minute of steam treatment.

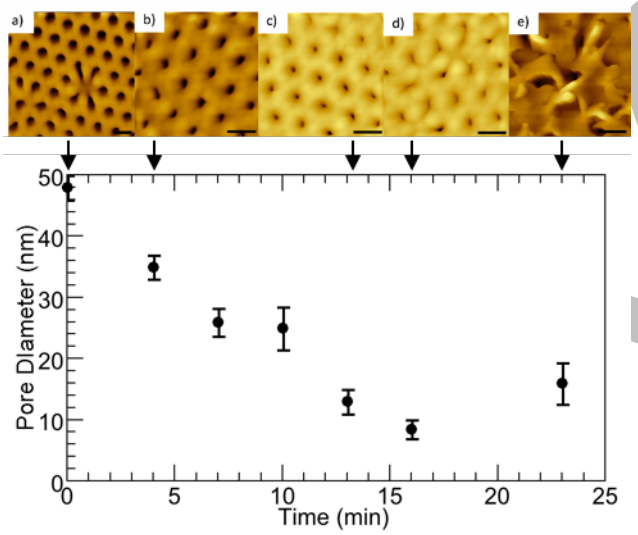

Fig. 6 Top: AFM micrographs of the same 40 V, 0.3 M oxalic AAM treated under steam for incremental time steps. Bottom: AAM average pore diameter reduction over time. Beyond 16 minutes, fibres start to grow on the surface of the AAM, analogous to those observed in the electrochemical treatment experiments. Error bars obtained from standard deviation measured by the AFM on an area of 500 x 500 nm^2.

Although the steam treatment of nanoporous AAOs or AAMs has not been previously studied, the mechanism leading to hydration of anhydrous and crystalline γ-Al_2O_3 films – chemically analogous to those produced here[25] - with steam is well-known, with the formation of metastable boehmite or pseudo-boehmite phases, which can, in turn, convert to more stable gibbsite γ-$Al(OH)_3$, upon exposure to humidity.[32] This transformation occurs without significant thermal expansion coefficient changes which could lead to cracking of the oxide structure, as in other phase changes that occur for alumina at higher temperatures.[33] Although the hydration mechanism is similar to the hydrothermal case, steam is more reactive than water and a better heat transfer fluid.[32] This explains why steam is capable of swelling the whole length of the pore, rather than only the pore mouth, as in the case of boiling water (cfr. Fig. 3c and 5c for the water and steam case, respectively). This is crucial in achieving uniform pore size reduction along the whole pore.

Conclusions

In this work we have provided a novel approach to reduce the pore size of anodic alumina membranes down to 10 nm, while maintaining the superior mechanical robustness of membranes produced at larger pore sizes. This is based on decoupling the final pore size from the anodization parameters, using a post-anodization hydrothermal treatment. Of the 3 methods investigated, immersion in boiling water produced a restriction at the pore ends together with an increase in roughness at the membrane surface, leaving the inner part of the pore unaffected. Treatment in a boiling solution containing NaCl to detect pore restriction using an electrochemical method produced no visible pore shrinking but rather the formation of fibrous structures on both membrane surfaces. However, using a steam treatment process, pore size reduction up to 80% was achieved, with uniform reduction throughout the whole length of the membrane. These results will allow the fabrication of anodic aluminium films and anodic alumina membranes with a broader range of pores sizes coupled with higher mechanical robustness than what is currently possible.

Acknowledgements

The authors acknowledge the EPSRC (grant EP/G045798/1) for funding and for the NanoAccess FESEM/FIB facility at the University of Cardiff (grant EP/F056745/1). DM is grateful to the Royal Academy of Engineering for support through a Research Fellowship.

Notes and references

[a] Department of Chemical Engineering, University of Bath, BA27AY, UK. Email: d.mattia@bath.ac.uk

1. J. P. O'Sullivan and G. C. Wood, *Proceed. R. Soc. Lond.*, 1970, **317**, 511-543.
2. C. Bae, H. Yoo, S. Kim, K. Lee, J. Kim, M. M. Sung and H. Shin, *Chem. Mater.*, 2008, **20**, 756-767.
3. C. R. Martin, *Science*, 1994, 1961-1966.
4. M. Steinhart, R. B. Wehrspohn, U. Gösele and J. H. Wendorff, *Angew. Chem., Int. Ed.*, 2004, **43**, 1334-1344.
5. G. D. Sulka, in *Nanostructured Materials in Electrochemistry*, ed. A. Eftekhari, Wiley-VCH, Weinheim2008.
6. O. Jessensky, F. Muller and U. Gosele, *J. Electrochem. Soc.*, 1998, **145**, 3735-3740.
7. M. Lillo and D. Losic, *J. Membr. Sci.*, 2009, **327**, 11-17.
8. K. P. Lee, H. Leese and D. Mattia, *Nanoscale*, 2012, **4**, 2621-2627.
9. H. Leese and D. Mattia, *Microfluid. Nanofluid.*, 2014, **16**, 711-719.
10. D. I. Petukhov, K. S. Napolskii and A. A. Eliseev, *Nanotechnology*, 2012, **23**, 335601.
11. D. I. Petukhov, K. S. Napolskii, M. V. Berekchiyan, A. G. Lebedev and A. A. Eliseev, *Acs Applied Materials & Interfaces*, 2013, **5**, 7819-7824.

12. H. Leese, V. Bhurtun, K. P. Lee and D. Mattia, *Colloids and Surfaces A: Physicochemical and Engineering Aspects*, 2013, **420**, 53-58.
13. C. Ran, G. Ding, W. Liu, Y. Deng and W. Hou, *Langmuir*, 2008, **24**, 9952-9955.
14. G. A. Pilkington, E. Thormann, P. M. Claesson, G. M. Fuge, O. J. L. Fox, M. N. R. Ashfold, H. Leese, D. Mattia and W. H. Briscoe, *Physical Chemistry Chemical Physics*, 2011, **13**, 9318-9326.
15. B. Quignon, G. A. Pilkington, E. Thormann, P. M. Claesson, M. N. R. Ashfold, D. Mattia, H. Leese, S. A. Davis and W. H. Briscoe, *ACS Nano*, 2013, **7**, 10850–10862.
16. P. Guo, C. R. Martin, Y. Zhao, J. Ge and R. N. Zare, *Nano Lett.*, 2010, **10**, 2202-2206.
17. T. Yanagishita, R. Fujimura, K. Nishio and H. Masuda, *Langmuir*, 2009, **26**, 1516-1519.
18. K. Nielsch, J. Choi, K. Schwirn, R. B. Wehrspohn and U. Gosele, *Nano Lett.*, 2002, **2**, 677-680.
19. V. Vega, V. Prida, M. Hernández-Vélez, E. Manova, P. Aranda, E. Ruiz-Hitzky and M. Vázquez, *Nanoscale Research Letters*, 2007, **2**, 355-363.
20. W. Lee, K. Schwirn, M. Steinhart, E. Pippel, R. Scholz and U. Gosele, *Nat Nano*, 2008, **3**, 234-239.
21. K. P. Lee and D. Mattia, *J. Membr. Sci.*, 2013, **435**, 52-61.
22. C. Y. Han, G. A. Willing, Z. Xiao and H. H. Wang, *Langmuir*, 2006, **23**, 1564-1568.
23. M. Lillo and D. Losic, *Mater. Lett.*, 2009, **63**, 457-460.
24. *Anodic oxidation of aluminium and its alloys*, Aluminium Federation1961.
25. G. Patermarakis, K. Moussoutzanis and J. Chandrinos, *App Catal A: General*, 1999, **180**, 345-358.
26. G. Boisier, N. Pébère, C. Druez, M. Villatte and S. Suel, *J. Electrochem. Soc.*, 2008, **155**, C521-C529.
27. J. Lee, U. Jung, W. Kim and W. Chung, *Appl. Surf. Sci.*, 2013, **283**, 941-946.
28. V. López, M. J. Bartolomé, E. Escudero, E. Otero and J. A. González, *J. Electrochem. Soc.*, 2006, **153**, B75-B82.
29. S. Feliu, Jr., J. A. González, V. López, M. J. Bartolome, E. Escudero and E. Otero, *Journal of Applied Electrochemistry*, 2007, **37**, 1027-1037.
30. H. Masuda and K. Fukuda, *Science*, 1995, **268**, 1466-1468.
31. G. Patermarakis and P. Kerassovitou, *Electrochim. Acta*, 1992, **37**, 125-131.
32. *Aqueous Systems at Elevated Temperatures and Pressures*, Academic Press2004.
33. H. C. Stumpf, A. S. Russell, J. W. Newsome and C. M. Tucker, *Industrial and Engineering Chemistry*, 1950, **42(7) pp 1398 - 1403**.